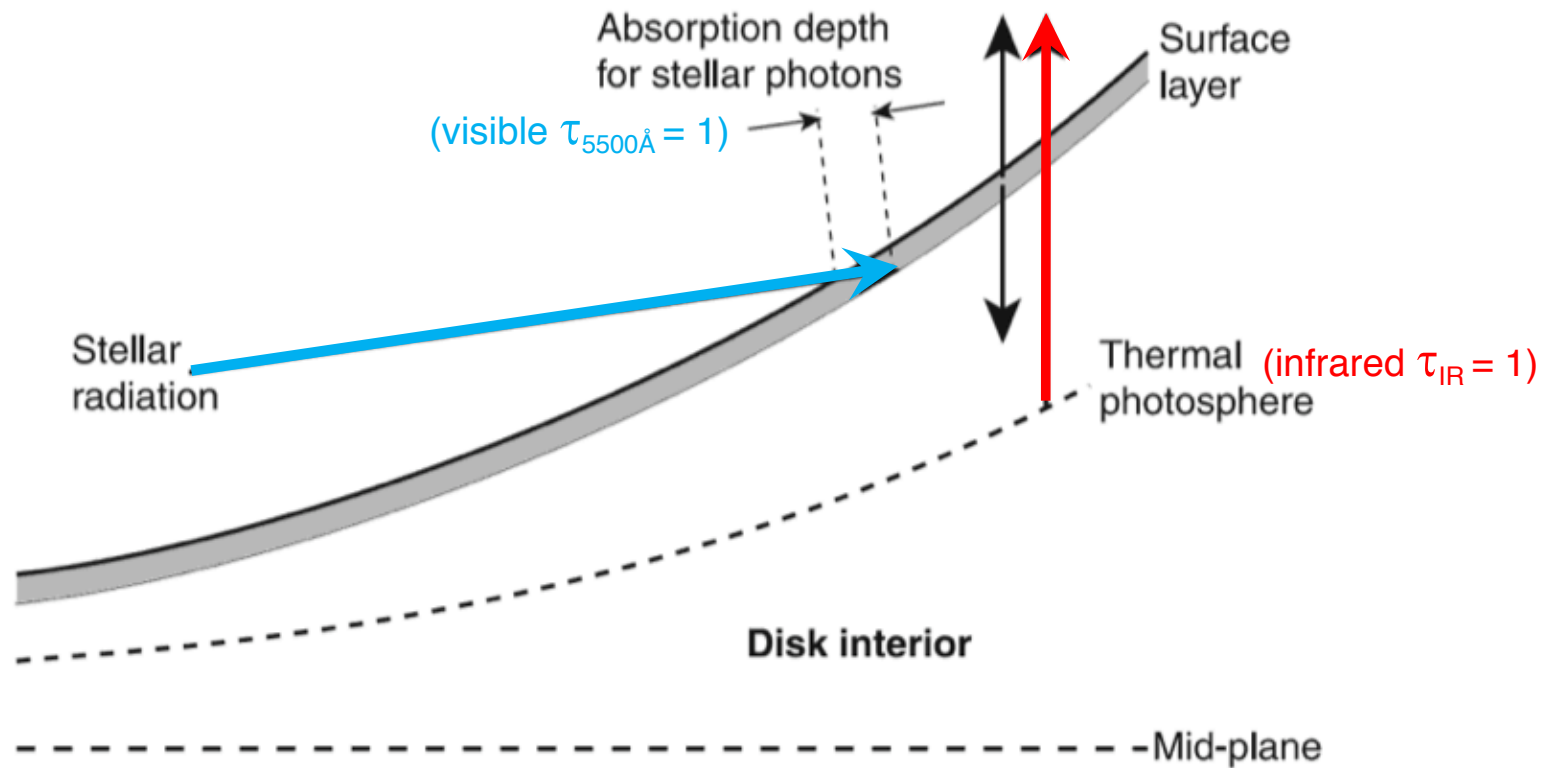


Radiative Equilibrium of Passive Disks



Radiative Equilibrium of Passive Disks

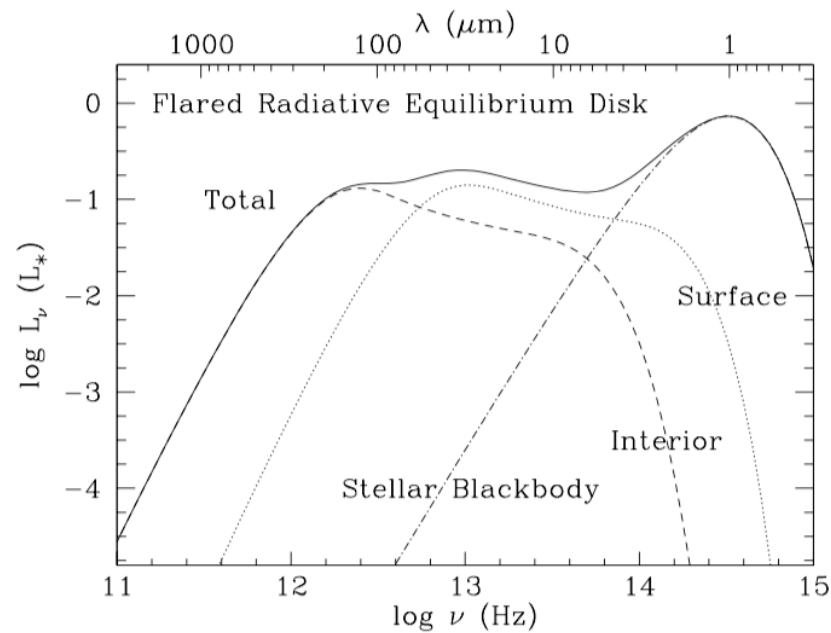


FIG. 6.—SED for the hydrostatic, radiative equilibrium disk. At mid-IR wavelengths, the superheated surface radiates approximately 2–3 times more power than the interior. Longward of $300 \mu\text{m}$, n gradually steepens from about 3 to $3 + \beta$ as the disk becomes increasingly optically thin.

Fit to GM Aur

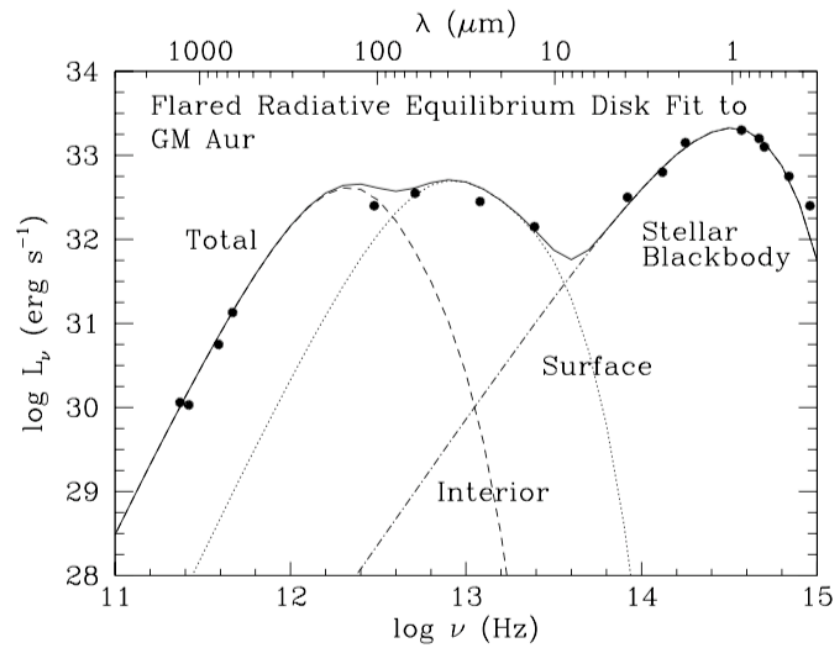
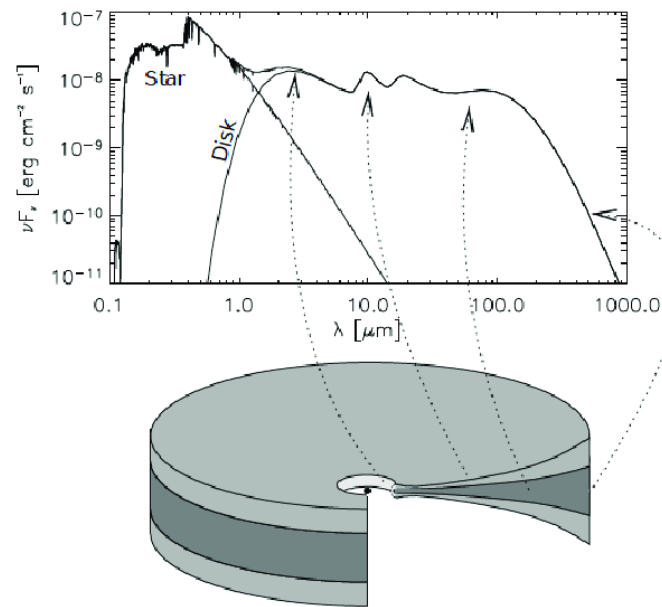


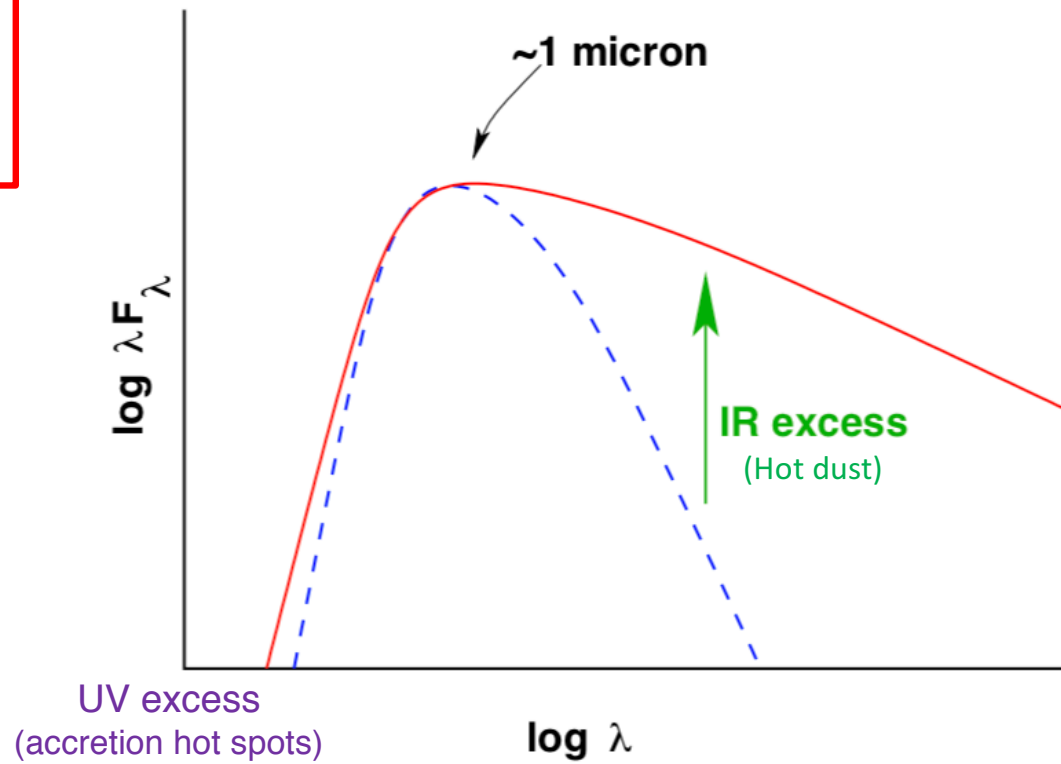
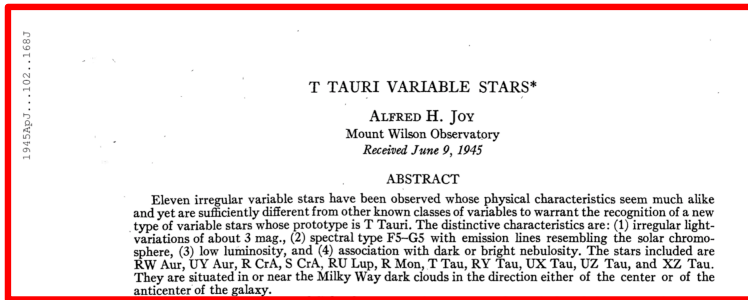
FIG. 8.—Observed SED of GM Aur (*filled circles*) and accompanying hydrostatic, radiative equilibrium (face-on) disk model. Fit parameters are as follows: $\Sigma = 3 \times 10^3 a_{\text{AU}}^{-3/2} \text{ g cm}^{-2}$, $\beta = 1.4$, $r_p = 0.3 \text{ } \mu\text{m}$, $a_o = 390 \text{ AU}$, and $a_i = 6.8 \text{ AU}$. The derived inner cutoff radius is likely an artifact of fitting a face-on model to a disk observed at substantial inclination (see the text for a discussion).

Disks are **optically thick** in **infrared**
and **optically thin** in **millimeter**



To witness planet formation we must observe in millimeter

T Tauri



UV Excess

Accretion Luminosity and Mass Accretion Rate

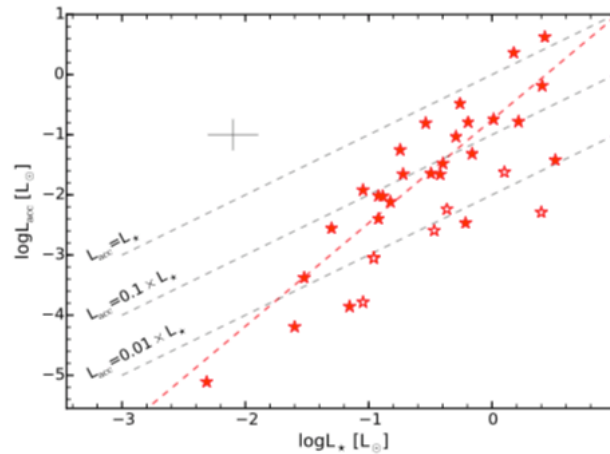


Fig. 4: Accretion luminosity as a function of stellar luminosity for the whole Chamaeleon I sample discussed here (*red stars*). Empty symbols denote non-accreting objects. Dashed lines are for different L_{acc}/L_{\star} ratios in decreasing steps from 1, to 0.1, to 0.01, as labeled. The best-fit relation from Eq. (2) is overplotted with a dashed red line. Typical uncertainties are shown in the upper left corner of the plot.

$$\log L_{\text{acc}} = (1.72 \pm 0.18) \cdot \log L_{\star} - (0.75 \pm 0.16)$$

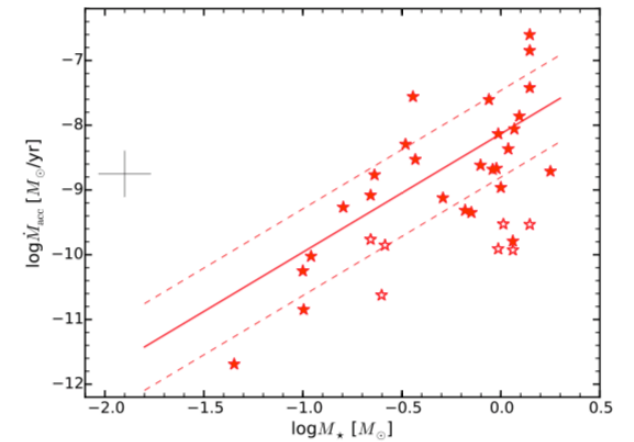


Fig. 6: Mass accretion rate as a function of the stellar mass for the whole Chamaeleon I sample discussed here (*red stars*). Empty symbols are used for non-accreting objects. The best-fit relation from Eq. (5) is overplotted with a red line, and the standard deviation from the best fit is shown with dashed lines. Typical uncertainties are shown in the upper left corner.

$$\log \dot{M}_{\text{acc}} = (1.83 \pm 0.35) \cdot \log M_{\star} - (8.13 \pm 0.16)$$

X-Shooter study of accretion in Chamaeleon I*

C.F. Manara^{1,*,*}, D. Fedele^{2,3}, G.J. Herczeg⁴, and P.S. Teixeira⁵

¹ Scientific Support Office, Directorate of Science and Robotic Exploration, European Space Research and Technology Centre (ESA/ESTEC), Keplerlaan 1, 2201 AZ Noordwijk, The Netherlands
e-mail: cmanara@cosmos.esa.int

² INFN-Osservatorio Astronomico di Arcetri, L.go F. Fermi 5, I-50125 Firenze, Italy

³ Max-Planck Institut für Extraterrestrische Physik, Giesenbachstrasse 1, 85748 Garching, Germany

⁴ Kavli Institute for Astronomy and Astrophysics, Peking University, Yi He Yuan Lu 5, Haidian Qu, Beijing 100871, China

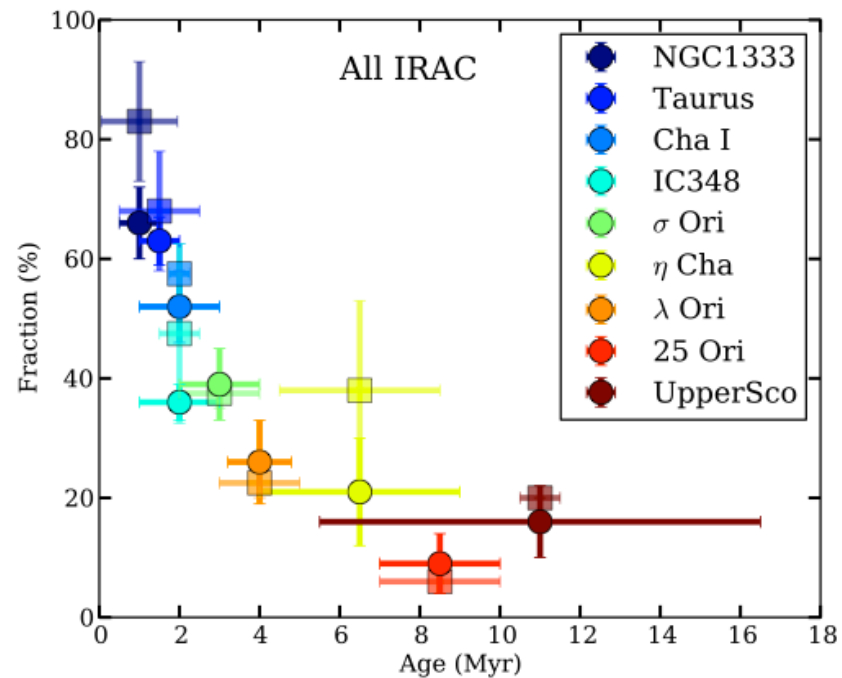
⁵ Universität Wien, Institut für Astrophysik, Türkenschanzstrasse 17, 1180 Vienna, Austria

Received August 21, 2015; accepted October, 23, 2015

ABSTRACT

We present the analysis of 34 new VLT/X-Shooter spectra of young stellar objects in the Chamaeleon I star-forming region, together with four more spectra of stars in Taurus and two in Chamaeleon II. The broad wavelength coverage and accurate flux calibration of our spectra allow us to estimate stellar and accretion parameters for our targets by fitting the photospheric and accretion continuum emission from the Balmer continuum down to ~ 700 nm. The dependence of accretion on stellar properties for this sample is consistent with previous results from the literature. The accretion rates for transitional disks are consistent with those of full disks in the same region. The spread of mass accretion rates at any given stellar mass is found to be smaller than in many studies, but is larger than that derived in the Lupus clouds using similar data and techniques. Differences in the stellar mass range and in the environmental conditions between our sample and that of Lupus may account for the discrepancy in scatter between Chamaeleon I and Lupus. Complete samples in Chamaeleon I and Lupus are needed to determine whether the difference in scatter of accretion rates and the lack of evolutionary trends are not influenced by sample selection.

Disk lifetime



(Ribas et al. 2014)



Disks dissipate within ~10Myr

A static description cannot be the full picture: **disks must evolve in time.**

Evolution summary (Spitzer Core to Disk Legacy)

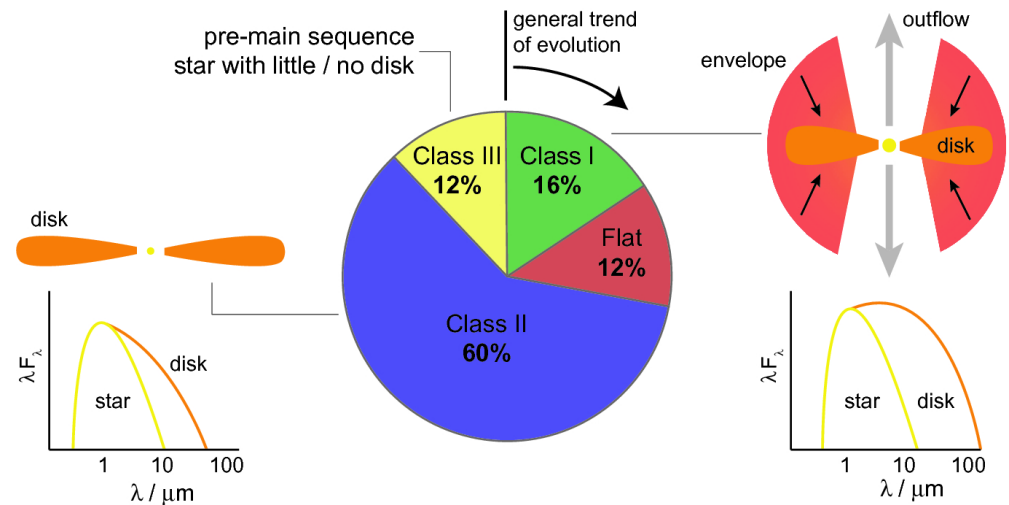
THE ASTROPHYSICAL JOURNAL SUPPLEMENT SERIES, 181:521–550, 2009 April
 © 2009. The American Astronomical Society. All rights reserved. Printed in the U.S.A.
 doi:10.1088/0067-0049/181/2/521

THE *SPITZER* c2d LEGACY RESULTS: STAR-FORMATION RATES AND EFFICIENCIES; EVOLUTION AND LIFETIMES

NEAL J. EVANS II¹, MICHAEL M. DUNHAM¹, JES K. JØRGENSEN², MELISSA L. ENOCH^{3, 4}, BRUNO MERÍN^{5, 6}, EWINE F. VAN DISHOECK^{5, 7}, JUAN M. ALCALÁ⁸, PHILIP C. MYERS⁹, KARL R. STAPELFELDT¹⁰, TRACY L. HUARD^{9, 11}, LORI E. ALLEN⁹, PAUL M. HARVEY¹, TIM VAN KEMPEN⁵, GEOFFREY A. BLAKE¹², DAVID W. KOERNER¹³, LEE G. MUNDY¹¹, DEBORAH L. PADGETT¹⁴, AND ANNEILA I. SARGENT³

¹ Department of Astronomy, University of Texas at Austin, 1 University Station C1400, Austin, TX 78712, USA; nje@astro.as.utexas.edu, mdunham@astro.as.utexas.edu, pmh@astro.as.utexas.edu
² Argelander Institut für Astronomie, University of Bonn, Auf dem Hügel 71, 53121 Bonn, Germany; jes@astro.uni-bonn.de
³ Division of Physics, Mathematics, and Astronomy, MS 105-24, California Institute of Technology, Pasadena, CA 91125, USA; afs@astro.caltech.edu
⁴ University of California, Berkeley, CA, USA
⁵ Leiden Observatory, Leiden University, P.O. Box 9513, NL 2300 RA Leiden, The Netherlands; ewine@strw.leidenuniv.nl
⁶ Research and Scientific Support Department, European Space Agency (ESTEC), P.O. Box 299, 2200 AG Noordwijk, The Netherlands; bmerin@rssd.esa.int
⁷ Max-Planck-Institut für Extraterrestrische Physik (MPE), Giessenbachstr. 1, 85748 Garching, Germany
⁸ INFN-OA Capodimonte, via Moianello 16, 80131 Naples, Italy; alcala@oa.cnr.it
⁹ Harvard-Smithsonian Center for Astrophysics, 60 Garden Street, Cambridge, MA 02138, USA; leallen@cfa.harvard.edu, pmyers@cfa.harvard.edu
¹⁰ Jet Propulsion Laboratory, MS 183-900, California Institute of Technology, Pasadena, CA 91109, USA; krs@exoplanet.jpl.nasa.gov
¹¹ Department of Astronomy, University of Maryland, College Park, MD 20742, USA; thuard@astro.umd.edu, lgm@astro.umd.edu
¹² Division of Geological and Planetary Sciences, MS 150-21, California Institute of Technology, Pasadena, CA 91125, USA; gab@gps.caltech.edu
¹³ Department of Physics and Astronomy, Northern Arizona University, NAU Box 6010, Flagstaff, AZ 86011-6010, USA; david.koerner@nau.edu
¹⁴ Spitzer Science Center, MC 220-6, California Institute of Technology, Pasadena, CA 91125, USA; djp@ipac.caltech.edu

Received 2008 August 2; accepted 2008 November 3; published 2009 March 11



Class II is the (main) epoch of planet formation